Proceedings of the 21st ICSMGE, Vienna, Austria, 14 – 19 June 2026. Pistrol, Adam & Schweiger (eds.)
Published by: ÖGG, Austrian Society for Geomechanics, Salzburg, Austria, ISBN 978-3-9503898-4-5
https://doi.org/10.53243/ICSMGE2026-1545

Soil densification with rigid inclusions for liquefaction mitigation

Catalina Mancilla
Arcadis, Chile, catalina.mancilla@arcadis.com

Patricio Donoso, Oscar Taiba
Ferrara Proyectos Especiales, Chile

Ana Belén Martínez Bacas, Pablo Ruiz-Terán
Ferrovial Construction, Spain

ABSTRACT: This study evaluates the effectiveness of ground improvement through rigid inclusions to mitigate liquefaction risk, based on numerical modeling and comparison with theoretical and empirical methods. The results confirm that the location of the rigid inclusion has a significant influence on the cyclic resistance ratio (CRR). Ground densification shows a noticeable improvement effect only when volumetric strain exceeds 1%.

Numerical simulations performed with Plaxis 2D demonstrate that, in the vicinity of the inclusion, the soil exhibits cap hardening and hardening point behavior, indicating an effective increase in both compressive and shear strength.

For the case studied, rigid inclusions are effective in reducing vulnerability parameters, as the Liquefaction Potential Index (LPI) and post-liquefaction settlements decrease from high to low levels.

When comparing methodologies, it was found that theoretical and empirical approaches tend to be less conservative than numerical analysis. Numerical models, evaluated in terms of volumetric strain or excess pore pressure and expressed as increases in CRR, FS, LPI, and post-seismic settlements, show strong agreement with each other.

To optimize design and ensure the effectiveness of improvement, it is recommended to combine multiple preliminary design methods and subsequently carry out in-situ measurements to verify that the target densification level has been achieved.

KEYWORDS: Liquefaction, rigid inclusions, densification, volumetric strain.

1 INTRODUCTION

Rigid inclusions as a ground improvement technique are a widely used solution to increase bearing capacity and reduce settlements in soft or loose soils, without the need for excavation or material removal. They are constructed by installing concrete columns that laterally displace the surrounding soil, creating a reinforcement grid with high construction efficiency and low environmental impact.

In non-cohesive soils with liquefaction potential, the use of rigid inclusions acts on two key mechanisms: (i) soil densification, which increases resistance to liquefaction, and (ii) ground reinforcement, by reducing cyclic demand through the insertion of a stiffer material.

This study analyzes the densification effect generated by rigid inclusions, with the aim of identifying methods to estimate it, applied to a site located in central Chile.

2 FRAMEWORK

2.1 *Soil Liquefaction*

Liquefaction is a phenomenon of saturated granular soils that occur under seismic or cyclic loading in undrained conditions. According to Kramer (1996), this condition leads to a progressive increase in pore pressure, which reduces the effective stress between particles until their shear strength is nullified, leaving the soil in a suspended state.

This phenomenon is particularly relevant in loose, contractive, and saturated soils, where the application of cyclic stress generates significant deformations that compromise the stability of structures found on them.

2.2 *Evaluating Soil Liquefaction Potential*

One of the most widely used methods for estimating liquefaction potential is that proposed by Seed and Idriss (1971), known as the simplified method. This approach compares the cyclic resistance ratio of the soil (CRR) with the cyclic stress ratio induced by a seismic event (CSR).

The analysis is carried out through empirical correlations based on historical case studies of sites that did or did not experience liquefaction, as a function of in situ parameters obtained from tests such as the Standard Penetration Test (SPT) or the Cone Penetration Test (CPT), while considering correction factors for depth, overburden stress, and earthquake magnitude. The factor of safety (FS) is defined as:

$$FS = \frac{CRR}{CSR} = \frac{CRR_{7.5}}{CSR} MSF * K_\sigma \quad (1)$$

Where:

- CRR: Cyclic resistance ratio.
- CSR: Cyclic stress ratio
- CRR7.5: Cyclic resistance ratio for an earthquake magnitude 7.5.
- MSF: Magnitude scale factor
- K_σ : Overburden stress correction factor

Several modifications to the method have been proposed; one of the most recent is the approach by Boulanger and Idriss (2014), which is applicable to both SPT and CPTu tests, and is the one adopted for the present analysis.

2.3 *Vulnerability parameters*

The Liquefaction Potential Index (LPI), proposed by Iwasaki, Tokida and Tatsuoka (1981), is used to quantify the severity of

liquefaction along the soil profile with depth. Its calculation is typically performed from the ground surface to a depth of 20 m, integrating the contribution of liquefiable layers based on their resistance and location.

$$LPI = \int_0^{20} (10 - 0.5 * z) * F_L * d_z \quad (2)$$

$$\begin{cases} F_L = 1 - FS \text{ si FS } \leq 1 \\ F_L = 0 \qquad \text{si FS} > 1 \end{cases} \quad (3)$$

The LPI is defined as such that higher values indicate greater severity and potential damage due to liquefaction. For practical interpretation, risk categories have been established based on the value obtained, which are summarized in Table 1.

Table 1. LPI Categories (Iwasaki, Tokida and Tatsuoka, 1981).

LPI	Category
0	Very low liquefaction potential: detailed studies are not required.
0 < LPI ≤ 5	Low liquefaction potential: studies are recommended for large structures.
5 < LPI ≤ 15	High liquefaction potential: liquefaction studies are necessary.
15 < LPI	Very high liquefaction potential: liquefaction studies are necessary.

The estimation of post-liquefaction settlements proposed by Zhang, Robertson and Brachman (2002) is obtained using the following relation:

$$S = \sum_{i=1}^{j} \varepsilon_{vi} \Delta z_i \quad (4)$$

Where:

- S: Post-liquefaction settlement
- ε_{vi}: Post-liquefaction volumetric strain in layer *i*.
- Δz_i: Thickness of layer i.

3 CASE STUDY

3.1 *Background*

The analyzed site is in central Chile. The average stratigraphy of the soil profile is detailed in Table 2. Notable features include the presence of superficial artificial fills and sand deposits with varying degrees of compaction overlying a rock basement at greater depth.

Table 2. General Stratigraphy.

Strate	Depth m	Description
H1	0.0 to 2.0	Artificial fill composed of sand and gravel with very loose compaction.
H2	2.0 to 38.0	Coarse sand, approximate grain size distribution: 0–2% gravel, 90–88% sand, 10% fines; light brown to gray color; odorless; zero plasticity; compaction ranging from loose to dense; homogeneous structure; low to medium cementation; no organic material detected.
H3	38.0 to 45.0	Good quality rock, light brown color, average RQD of 78%.
Groundwater table		4.0 m depth

The liquefaction potential was evaluated using the method by Boulanger and Idriss (2014) based on a CPTu test analyzed with the CLiq software. Parameters considered for the analysis are summarized in Table 3, with liquefaction assessment limited to a depth of 20.0 m. Figure 1 shows the factor of safety results and vulnerability parameters for the case study.

Table 3. Parameters for liquefaction analysis.

Mw	PGA g	Water table in situ m	Water table design m
8.8	0.57	4.0	3.0

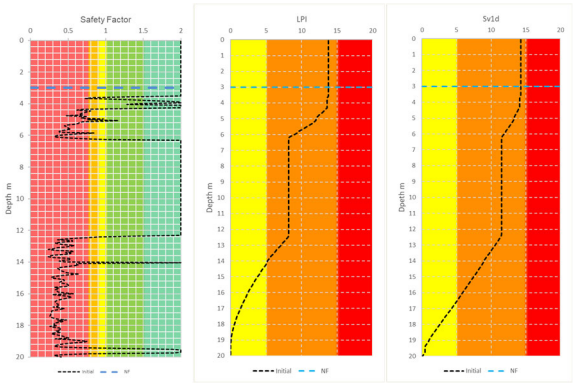

Figure 1. Liquefaction Potential Assessment without Ground Improvement (CPTu method).

3.2 *Ground Improvement*

As a mitigation measure against liquefaction susceptibility, the implementation of rigid inclusions 36 cm in diameter is proposed, extending to a depth of 20 m. The columns are arranged in a triangular (staggered) grid with a spacing of 1.7 m center-to-center, designed to provide uniform and efficient coverage of the susceptible soil.

4 METHODOLOGY AND RESULTS

4.1 *Theoretical Approach Based on Relative Density*

4.1.1 *Methodology*

The evaluation of the ground improvement effect is performed through a theoretical approach based on changes in the relative density of the granular soil. For a triangular arrangement of rigid inclusions, the equivalent diameter (d_e) is defined as 1.05×s, where s is the center-to-center spacing between columns. The final total volume (V_{tf}) corresponding to the soil volume with inclusions is calculated by the following expression:

$$V_{tf} = \pi \left(\frac{1.05\, s}{4}\right)^2 L - \pi r_c^2 L \quad (5)$$

Under the hypothesis of constant solids volume (V_s) the relation between initial and final void ratios is given by:

$$e_f = \frac{V_{tf}}{V_{ti}}(1 + e_i) - 1 \quad (6)$$

The relative density (DR) is estimated from the cone tip resistance obtained in CPTu tests using the correlation proposed by Baldi, Belloti, Ghionna, Jamiolkowski and Lo Presti (1989), as referenced by Robertson and Cabal (2014):

$$DR = \left(\frac{1}{C_2}\right) ln\left(\frac{Q_{cn}}{C_0}\right) \quad (7)$$

Where, C_0=15.7 and C_2=2.41 are soil constants for normally consolidated sands, Q_{cn} is the cone resistance normalized by atmospheric pressure (p_a=101 kPa) and vertical effective stress(σ'_{v0}).

Additionally, the improvement factor (n) is defined as:

$$n = \frac{q_{cf}}{q_{ci}} \quad (8)$$

4.1.2 *Results*

Figure 2 presents the improvement factor values as a function of depth. These values were incorporated into the CLiq software for re-evaluation of the liquefaction potential, adjusting the soil resistance values (q_t). Figure 3 shows safety factors, vulnerability indicators at the surface exhibit a significant reduction in liquefaction risk.

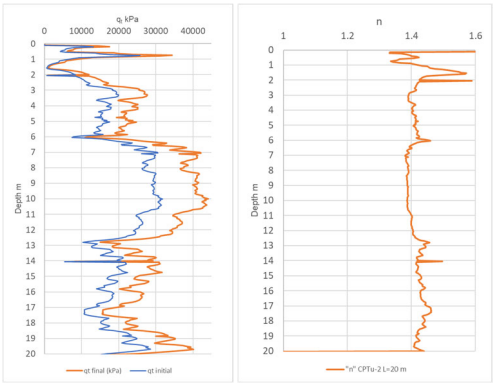

Figure 2. Cone resistance and improvement factor, RD method.

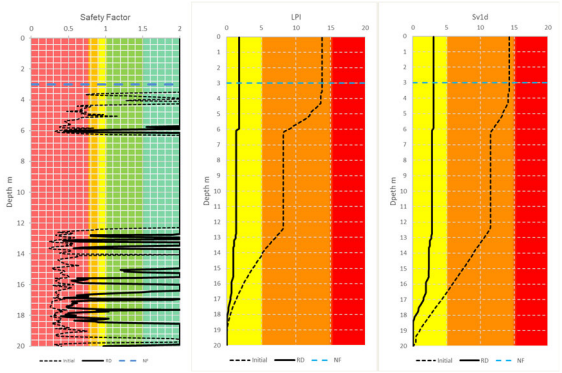

Figure 3. CLiq Results, RD Method.

4.2 *Previous Experiences*

4.2.1 *Methodology*

Table 4 presents the values reported by Varaksin (2010), which provide an improvement factor based on soil type (grain size distribution) and the percentage of replacement area used, to estimate the improvement factor (n).

Table 4. Improvement Factor (Varaksin, 2010).

Replacement Area [%]	Improvement Factor (n)		
	Sand	Silt	Clay
1.0	1.3	1.2	1.1
2.0	1.5	1.4	1.2
4.0	2.0	1.6	1.3

4.2.2 *Results*

Considering that the soil is predominantly sand with low fines content, and that the replacement area is 4%, according to Table 4 the improvement factor is taken as 2.0. Figure 4 shows the improved soil values, and Figure 5 presents the results obtained with the CLiq software.

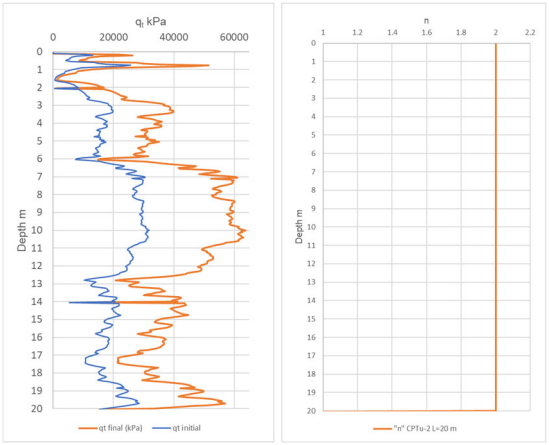

Figure 4. Cone resistance and improvement factor, previous Experience method.

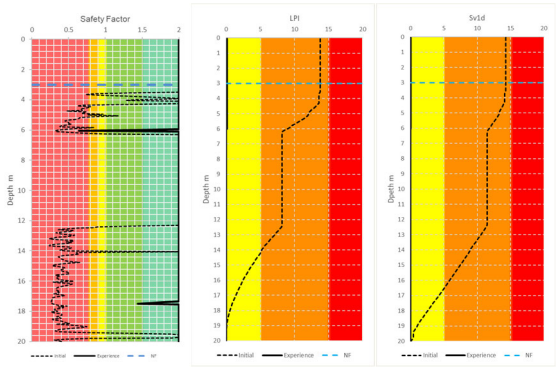

Figure 5. CLiq Results, Previous Experience Method.

4.3 *Numerical modeling with Plaxis 2D*

4.3.1 *Model and geometry*

The stress-strain behavior of the granular soil is simulated using the Hardening Soil constitutive model with isotropic hardening, while the rigid inclusions are represented with a linear elastic model. The parameters were estimated from empirical correlations with CPTu test records, summarized in Table 5. The parameters adopted for the rigid inclusions are presented in Table 6.

Table 5. Parameters Adopted for the Hardening Soil Model.

Parameters	H1	H2	H3
$\gamma_{un\,sat}$ /γ_{sat} kN/m^3	16.0/17.0	18.0/19-0	19.0/20.0
$E_{50}{}^{ref}$ MPa	24	50	55
$E_{eod}{}^{ref}$ MPa	24	50	55
$E_{ur}{}^{ref}$ MPa	72	150	165
p^{ref} kPa	100	100	100
m	0.5	0.5	0.5
c' kPa	0.0	0.0	0.0
ϕ' °	30	38	38
ψ °	0	5	5
R_f	0.9	0.9	0.9

Table 6. Adopted for the Rigid Inclusions Using the Linear Elastic Model.

E GPa	γ_{sat} kN/m^3
15.0	24.0

4.3.2 *Evaluation of Post-Improvement Cyclic Resistance of Soil (CRR)*

According to the proposal by O'Sullivan, Terzaghi and Orense (2014), the installation of rigid columns induces volumetric deformation of the ground, which results in an increase in the effective confinement stress (σ'_3), generating an increase in the coefficient of earth pressure at rest (K_0). This coefficient corresponds to the ratio between effective horizontal and vertical stresses. This increase translates into two effects:

- Reduction of the initial stress state.
- Increase in the soil shear strength.

To quantify the effect of the increase in earth pressure coefficient (K_0) on the evaluation of liquefaction potential, the relationship from Salgado, Boulanger and Mitchell (1997) is used to quantify the post-improvement cyclic shear resistance ($CRR_{Post\ IC}$) after column installation:

$$CRR_{Post\ IC} = CRR_i \frac{(1 + 2K_{0\ Post\ IC})}{(1 + 2K_{0\ i})} \quad (8)$$

Where $K_{0\ Post\ IC}$ s the earth pressure coefficient after column installation, and $K_{0\ i}$ is the initial earth pressure coefficient (without improvement).

To evaluate the spatial effect of the induced confinement, three radial locations relative to the column axis were analyzed (r= 0.2m, 0.5m, and 0.9m), recording the evolution of the horizontal-to-vertical stress ratio with depth (Figure 6).

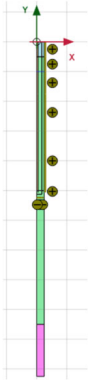

Figure 6. Axisymmetric Plaxis 2D Model.

Two numerical modeling approaches were implemented in Plaxis 2D under axisymmetric conditions:

- Volumetric deformation
- Injection pressure

4.3.3 *Volumetric Deformation*

An axisymmetric model was used to evaluate the principal stress ratio under different levels of volumetric deformation induced by soil improvement: 0.2%, 0.64%, 1%, and 5%, comparing initial conditions and post-rigid inclusion. Figure 7 presents one of the analyzed cases (r= 0.2 m, e_v= 5%), showing that a linear correlation allows obtaining K_0 for both conditions.

This analysis was performed for all cases, and the ratio between post- and pre-improvement CRR was calculated according to Equation (8). The results for each case are presented in Table 6.

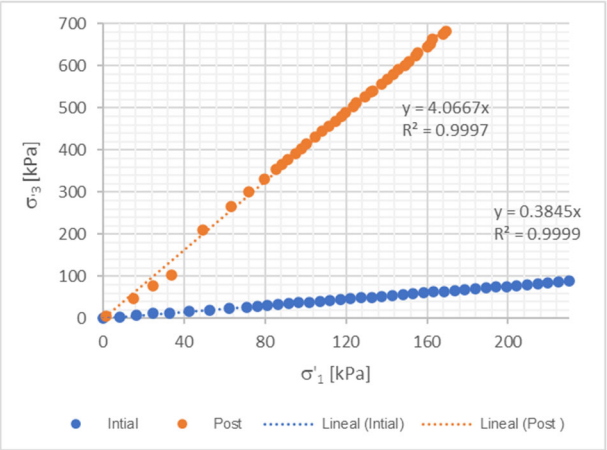

Figure 7. Case r=0.2m e_v=5% Relationship between principal strains to obtain earth pressure coefficient before and after rigid inclusion.

Table 7. Increase in CRR from Volumetric Deformation Modeling.

Volumetric Deformation %	$CRR_{Post}/CRR_{Initial}$		
	0.2 m	0.5 m	0.9 m
0.20	1.42	1.08	1.03
0.64	2.14	1.27	1.12
1.0	2.53	1.41	1.17
5.0	5.12	2.86	1.87

4.3.4 *Injection Pressure*

This approach simulates the construction process of rigid inclusions by applying injection pressure to reproduce the radial thrust exerted on the soil during installation. In the axisymmetric model, internal pressures were applied at the contact nodes between the column and soil, evaluating three representative levels: 200 kPa, 400 kPa, and 1000 kPa.

A depth-variable load was used to prevent soil failure, since pressures above 200 kPa may cause instability issues. Figure 8a shows the load application, and Figure 8b presents the total volumetric deformation associated.

Table 7 shows result for the relative increase in cyclic resistance coefficient (CRR) at different evaluation radius (0.2 m, 0.5 m, and 0.9 m) from the column axis for each applied pressure level.

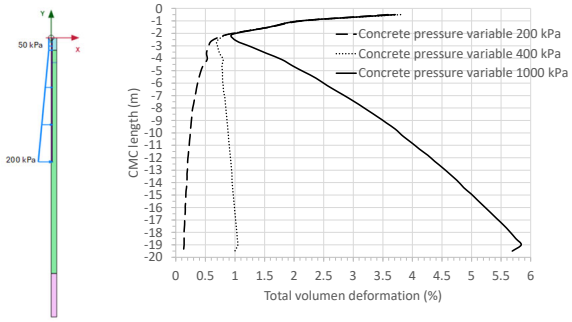

(a) (b)

Figure 8. (a) Load variable with the depth from 50 kPa until 200 kPa or 400 kPa or1000 kPa. (b) Volumetric deformation.

Table 8. Increase in CRR from Injection Pressure Modeling.

Pressure kPa	$CRR_{Post}/CRR_{Initial}$		
	0.2 m	0.5 m	0.9 m
200	1.00	1.00	1.04
400	2.42	1.32	1.16
1000	4.93	2.58	1.75

5 ANALYSIS RESULTS

5.1 *Comparison of results between models*

Figure 9 presents a comparative analysis of the increase in soil strength obtained from the different models, showing consistent agreement between cases with the same distance from the column and volumetric strain, which validates the coherence of the numerical model used. Additionally, a marked variation in the CRR increase is identified depending on the position relative to the rigid inclusion. For volumetric strains greater than 1%, the effect on strength becomes significant at all evaluated positions.

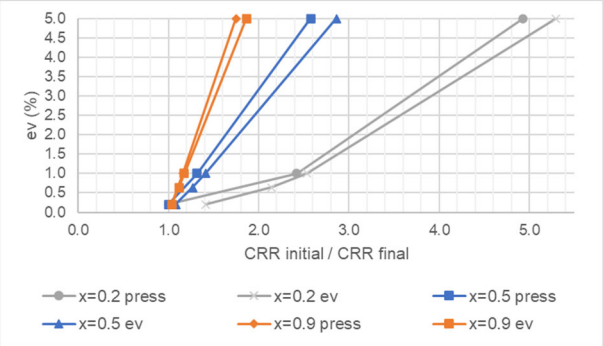

Figure 9. Comparison between Plaxis 2D models.

Figure 10 shows that in the immediate vicinity of the rigid inclusion, the soil behavior exhibits cap hardening and hardening point for volumetric strains of 0.2%, 1%, and 5%.

In the Hardening Soil model, cap hardening is associated with an increase in the preconsolidation pressure (Pp), reflecting an increase in soil strength against volumetric compression. The hardening point, on the other hand, relates to shear hardening, indicating the progressive mobilization of shear strength.

At the boundary of the column's influence area (r = 0.9 m), cap hardening is observed for strains of 0.2% and 1%, indicating a localized increase of Pp. When volumetric strain increases to 5%, the response transitions to a combined state of cap + hardening point. For strains on the order of 15%, a failure state is identified near the inclusion.

In terms of ground improvement, the objective is to maximize compaction hardening (increase in Pp) and minimize shear hardening as much as possible to avoid premature shear degradation.

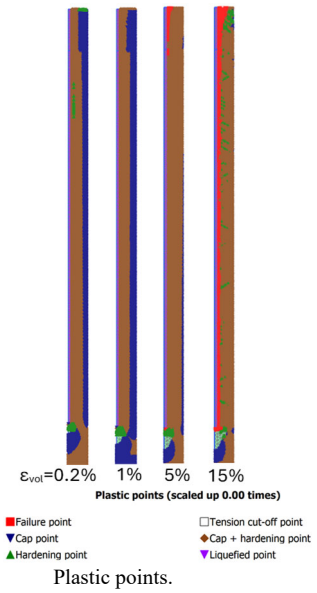

Figure 10. Plastic points.

5.2 *Safety Factor*

To compare the different methodologies, safety factors (SF) at a depth of 13 m are plotted in Figure 11. It is observed that densification varies significantly with position, and that theoretical or experience-based methods tend to be less conservative. Additionally, for volumetric strains below 1% (associated with pressures below 400 kPa), the increase in liquefaction resistance (CRR) is not significant.

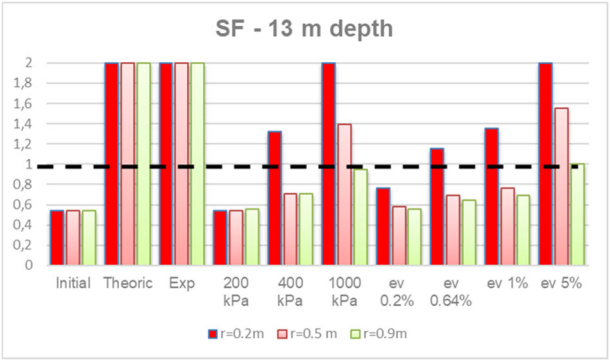

Figure 11. SF at 13 m depth.

5.3 *Vulnerability parameters*

According to the results shown in Figures 12 and 14, the analyzed methods succeed in reducing the Liquefaction Potential Index (LPI) and the post-liquefaction settlements from a high to a low level in most cases.

The finite element analysis is identified as the most conservative method, due to its ability to integrate a greater number of geotechnical factors. For liquefaction damage mitigation to be effective, it is crucial that a minimum volumetric strain of 1% is achieved.

The comparison of Plaxis models in Figures 13 and 15 confirms a strong agreement in the results of LPI and settlements when volumetric strains are considered. It is concluded that the densification effect becomes evident only for volumetric strains exceeding 1%.

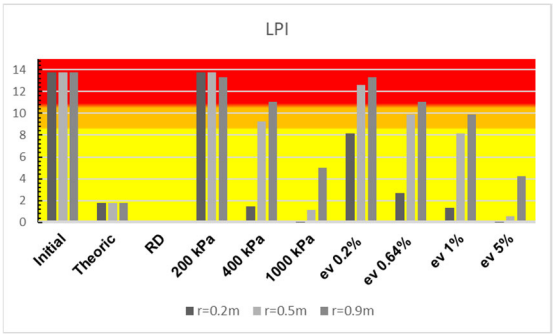

Figure 12. LPI Results.

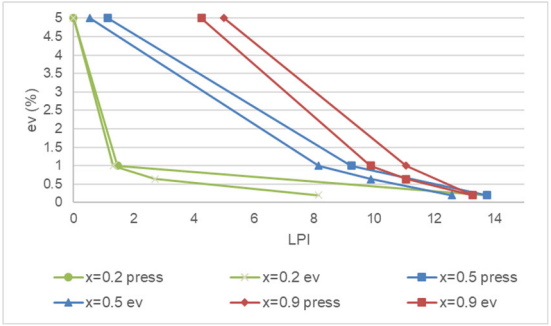

Figure 13. Comparison between Plaxis 2D models in terms of LPI.

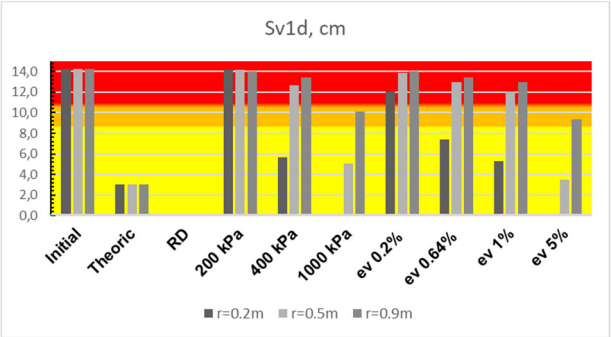

Figure 14. Post liquefaction settlement results.

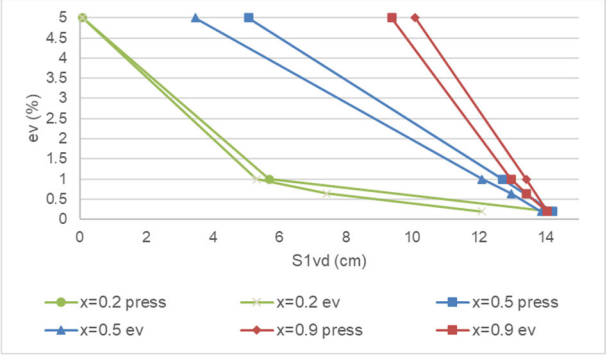

Figure 15. Comparison between Plaxis 2D models in terms of Post seismic liquefaction settlement.

6 CONCLUSIONS

- The results of the conducted simulations confirm that the location of the rigid inclusion significantly influences the increase in the cyclic resistance ratio (CRR).
- The comparison of methodologies reveals that methods based on previous experience or theoretical approaches tend to be less conservative. It is observed that densification varies significantly with position, and that the increase in liquefaction resistance (CRR) is marginal for volumetric strains below 1%, which are associated with pressures under 400 kPa.
- When comparing the numerical simulations performed in Plaxis in terms of CRR increase, factor of safety (FS), LPI, and settlement, a strong agreement is confirmed in the results when comparing models associated with a given volumetric strain.
- Plaxis 2D simulations show that near the rigid inclusion, the soil exhibits cap hardening and hardening point, corresponding to increased volumetric compression resistance and shear hardening, respectively. These phenomena are observed for volumetric strains between 0.2% and 5%. At 0.9 meters, cap hardening predominates with strains up to 1%, but with strains greater than 5%, a combined state of cap hardening and hardening point develops. This behavior indicates that the soil improvement method is effective, as it increases compression resistance (increase in preconsolidation pressure, Pp) and, at higher strains (15%), allows failure initiation around the inclusion. Ideally, to optimize improvement, compaction hardening should be maximized and shear hardening minimized to avoid premature shear failure.
- According to the analyzed results and various methodologies, regarding vulnerability parameters, the Liquefaction Potential Index (LPI) and post-liquefaction settlements decrease from high to low levels with the proposed improvement.
- As a design recommendation for densification estimation, it is suggested to use a combination of several methods for the preliminary design (all are relatively simple to apply). Subsequently, once the soil improvement has been performed, in situ measurements should be conducted to verify that the required densification level has been achieved.

7 REFERENCES

Baldi, G., Belloti, R., Ghionna, V. N., Jamiolkoski, M., & Lo Presti, D. C. F. (1989). Modulus of sands from CPT's and DMT's. In Proceedings of the 12th International Conference on Soil Mechanics and Foundation Engineering (pp. 165–170).

Boulanger, R., & Idriss, I. (2014). CPT and SPT based liquefaction triggering procedures (Technical report). University of California, Davis.

Iwasaki, T., Tokida, K. and Tatsuoka, F. (1981). Soil liquefaction potential evaluation with use of simplified procedures. 1st International Conference on Recent Advances in Geotechnical Earthquake Engineering & Soil Dynamics, 209-214.

Kramer, S. L. (1996). Geotechnical earthquake engineering. Prentice Hall.

O'Sullivan, A., Terzaghi, S., & Orense, R. (2014). The design of open grid Deep Soil Mixing (DSM) foundation on earthquake related projects. In Soil liquefaction during recent large-scale earthquakes. CRC Press.

Robertson, P. K., & Cabal, K. L. (2014). Guide to cone penetration testing for geotechnical engineering. Gregg Drilling & Testing.

Salgado, R., Boulanger, R. W., & Mitchell, J. K. (1997). Lateral stress effects on CPT liquefaction resistance correlations. Journal of Geotechnical and Geoenvironmental Engineering, 123(8), 726–735.

Seed, H. B., & Idriss, I. M. (1971). Simplified procedure for evaluating soil liquefaction potential. Journal of the Soil Mechanics and Foundation Division, 97(9), 1249–1973.

Varaksin, S. (2010). Concept and parameters with added material. Ground Improvement Workshop, Perth, Australia.

Zhang, G., Robertson, P. K., & Brachman, R. W. I. (2002). Estimating liquefaction-induced ground settlements from CPT from ground level. Canadian Geotechnical Journal, 39, 1168–1180.